

Susumu Uchiyama · Fumio Arisaka
Walter F. Stafford · Tom Laue *Editors*

Analytical Ultracentrifugation

Instrumentation, Software,
and Applications

 Springer

Analytical Ultracentrifugation

Susumu Uchiyama • Fumio Arisaka •
Walter F. Stafford • Tom Laue
Editors

Analytical Ultracentrifugation

Instrumentation, Software, and Applications

 Springer

Editors

Susumu Uchiyama
Graduate School of Engineering
Osaka University
Suita
Osaka, Japan

Fumio Arisaka
Life Science Research Center
Nihon University
Fujisawa
Kanagawa, Japan

Walter F. Stafford
Department of Neurology
Harvard Medical School
Boston
Massachusetts, USA

Tom Laue
BITC
University of New Hampshire
Durham
New Hampshire, USA

ISBN 978-4-431-55983-2 ISBN 978-4-431-55985-6 (eBook)
DOI 10.1007/978-4-431-55985-6

Library of Congress Control Number: 2016938115

© Springer Japan 2016

This work is subject to copyright. All rights are reserved by the Publisher, whether the whole or part of the material is concerned, specifically the rights of translation, reprinting, reuse of illustrations, recitation, broadcasting, reproduction on microfilms or in any other physical way, and transmission or information storage and retrieval, electronic adaptation, computer software, or by similar or dissimilar methodology now known or hereafter developed.

The use of general descriptive names, registered names, trademarks, service marks, etc. in this publication does not imply, even in the absence of a specific statement, that such names are exempt from the relevant protective laws and regulations and therefore free for general use.

The publisher, the authors and the editors are safe to assume that the advice and information in this book are believed to be true and accurate at the date of publication. Neither the publisher nor the authors or the editors give a warranty, express or implied, with respect to the material contained herein or for any errors or omissions that may have been made.

Printed on acid-free paper

This Springer imprint is published by Springer Nature
The registered company is Springer Japan KK

Preface

Analytical ultracentrifugation (AUC) is one of most powerful and reliable techniques to study the biophysical behavior of solutes in solution. Since 1950, there have been more than 16,000 references to analytical ultracentrifugation, including 17 books on the topic. In the last few years, there have been steady advances made in hardware, software, and applications for AUC. In this book, therefore, we focus on (1) providing chapters that cover everything essential for beginners to the most advanced users; (2) updating the field on advances in hardware, software, and applications; and (3) encompassing AUC applications for nonbiological questions.

The first two chapters (Chaps. 1 and 2) in Part 1 provide minimum but essential theoretical and experimental explanations for studies using AUC. In Part 2, novel analytical ultracentrifuge instrumentation (Chap. 3) and detection systems (Chaps. 4 and 5) that give added dimensions to AUC are introduced, followed by three chapters describing computer programs for sedimentation data analysis (Chaps. 6, 7 and 8). The final four chapters (Chaps. 9, 10, 11 and 12) in Part 2 introduce the theoretical and practical considerations for calculating hydrodynamic parameters, such as the sedimentation and diffusion coefficients, from three-dimensional molecular structure. The next three parts describe applications of AUC to specific research fields including material science (Part 3, Chaps. 13 and 14), membrane proteins (Chap. 15), protein–ligand interactions (Chap. 16), and polysaccharides (Chap. 18). Sedimentation analysis of high-salt-concentration solutions and the concomitant changes in chemical activity of biological macromolecules are introduced in Chap. 17. AUC for biopharmaceutical formulations, typically composed of proteins, buffers, salts, and additives such as sugars and surfactants, is introduced in three chapters of Part 5. First, the importance of AUC in the quantitation of oligomers and aggregates is introduced in Chap. 19. Next, Chap. 20 introduces practical approaches for the analysis of protein size distributions in biopharmaceuticals. Finally, methods for evaluating the intermolecular interactions that underlie protein behavior and govern protein aggregation by sedimentation equilibrium are presented in Chap. 21. Part 6 focuses on the AUC of high-concentration and complex systems, where hydrodynamic nonideality may influence sedimentation of macromolecules

strongly. Presented in this part are recent advances in AUC detectors and developments in programs for AUC data analysis that will enable us to use AUC under these highly nonideal conditions. Theory (Chap. 22), data acquisition, and data analysis (Chaps. 23, 24 and 25) are comprehensively described. Finally, Chap. 26 in Part 7 provides an example of new application of AUC for studies of biological macromolecules.

We are convinced that AUC will remain one of the most powerful biophysical methods, and, with the advances described here, will continue to grow in terms of theory, instrumentation, and data analysis.

Osaka, Japan
Fujisawa, Japan
Cambridge, MA, USA
Durham, NH, USA

Susumu Uchiyama
Fumio Arisaka
Walter F. Stafford
Tom Laue

Contents

Part I Introduction

- 1 Important and Essential Theoretical Aspects of AUC**..... 3
Susumu Uchiyama and Fumio Arisaka
- 2 Experimental Design and Practical Aspects** 15
Fumio Arisaka and Susumu Uchiyama

Part II AUC Instrumentation and Analysis

- 3 The CFA Analytical Ultracentrifuge Architecture**..... 25
Thomas M. Laue and J. Brett Austin
- 4 Fluorescence Detection System**..... 39
Tao G. Nelson, Glen D. Ramsay, and Matthew A. Perugini
- 5 The Multiwavelength UV/Vis Detector: New Possibilities
with an Added Spectral Dimension**..... 63
Engin Karabudak and Helmut Cölfen
- 6 SEDANAL: Model-Dependent and Model-Independent
Analysis of Sedimentation Data**..... 81
Peter J. Sherwood and Walter F. Stafford
- 7 SEDANAL: Global Analysis of General Hetero- and
Self-Associating Systems by Sedimentation Equilibrium** 103
Walter F. Stafford and Peter J. Sherwood
- 8 Analytical Ultracentrifugation Data Analysis with UltraScan-III** 119
Borries Demeler and Gary E. Gorbet

Part III Hydrodynamic Modeling

- 9 Introduction: Calculation of Hydrodynamic Parameters** 147
Olwyn Byron

10	Calculation of Hydrodynamic Parameters: US-SOMO	169
	Emre Brookes and Mattia Rocco	
11	The HYDRO Software Suite for the Prediction of Solution Properties of Rigid and Flexible Macromolecules and Nanoparticles	195
	José García de la Torre	
12	Accurate Hydrodynamic Modeling with the Boundary Element Method	219
	Sergio R. Aragon	
Part IV Applications of AUC: Material Science		
13	Hydrodynamic Analysis of Synthetic Permanently Charged Polyelectrolytes	251
	Christine Wandrey and Hamideh Ahmadloo	
14	Different Levels of Self-Sufficiency of the Velocity Sedimentation Method in the Study of Linear Macromolecules	269
	Georges M. Pavlov	
Part V Applications of AUC: Biological Science		
15	Applications of Analytical Ultracentrifugation to Membrane Proteins	311
	Karen G. Fleming	
16	Protein-Ligand Interactions	329
	Shane E. Gordon and Matthew A. Perugini	
17	AUC in the High Concentration of Salts/Cosolvent	355
	Christine Ebel	
18	Aspects of the Analytical Ultracentrifuge Determination of the Molar Mass Distribution of Polysaccharides	375
	Stephen E. Harding, Gary G. Adams, Richard B. Gillis, Fahad M. Almutairi, and Gordon A. Morris	
Part VI Applications of AUC: Biopharmaceuticals		
19	Use of Analytical Ultracentrifugation as an Orthogonal Method for Size Exclusion Chromatography: Assuring Quality for Therapeutic Protein Products and Meeting Regulatory Expectations	389
	John F. Carpenter, David L. Bain, and Gibbes R. Johnson	
20	Biopharmaceuticals: Application of AUC-SV for Quantitative Analysis of Protein Size Distributions	397
	Amanda A. Cordes, Kelly K. Arthur, and John P. Gabrielson	

21 Biopharmaceutical Evaluation of Intermolecular Interactions by AUC-SE	419
Shuntaro Saito and Susumu Uchiyama	
Part VII AUC of High-Concentration Systems and Non-ideal Solutions	
22 Johnston-Ogston Effects in Two Simulated Systems of Polystyrene Beads That Are Polydisperse with Respect to Density	443
Thomas P. Moody	
23 Analysis of Nonideal, Interacting, and Noninteracting Systems by Sedimentation Velocity Analytical Ultracentrifugation	463
Walter F. Stafford	
24 Techniques for Dissecting the Johnston-Ogston Effect	483
John J. Correia, Daniel F. Lyons, Peter Sherwood, and Walter F. Stafford	
25 Acquisition and Analysis of Data from High Concentration Solutions	499
Tabot M.D. Besong and Arthur J. Rowe	
Part VIII New Applications of AUC	
26 Detection and Quantitative Characterization of Macromolecular Heteroassociations via Composition Gradient Sedimentation Equilibrium	523
Allen P. Minton	

Part I
Introduction

Chapter 1

Important and Essential Theoretical Aspects of AUC

Susumu Uchiyama and Fumio Arisaka

Abstract Analytical ultracentrifugation (AUC) is a powerful method to reveal biophysical behavior of solute in solution. AUC has a long history and is based on well-established and concrete thermodynamic and hydrodynamic theory. AUC provides valuable parameters such as the sedimentation and diffusion coefficients, from which molar mass and information on hydrodynamic shape and solvation of the solute can be derived. Here, important and essential theoretical aspects of AUC are described.

Keywords Analytical ultracentrifugation • Sedimentation equilibrium • Sedimentation velocity • Theory

1.1 Introduction

This chapter is devoted to the basics of analytical ultracentrifugation. Efforts have been made to cover the minimum essentials and to make it qualitatively but precisely understandable. Two fundamentally important concepts in analytical ultracentrifugation are sedimentation and diffusion. Detailed theories can be found in the published literature (Fujita 1962; Cantor and Schimmel 1980; van Holde et al. 2005).

There are two modes of experiments, namely, sedimentation velocity (SV) and sedimentation equilibrium (SE). In SV experiments, both sedimentation and diffusion take place simultaneously. In SE experiments, sedimentation and diffusion are balanced and reach equilibrium.

S. Uchiyama (✉)

Department of Biotechnology, Graduate School of Engineering, Osaka University, 2-1 Yamadaoka, Suita, Osaka 565-0871, Japan

Department of Bioorganization Research, Okazaki Institute for Integrative Bioscience, 5-1 Higashiyama, Myodaiji-cho, Okazaki, Aichi 444-8787, Japan
e-mail: suchi@bio.eng.osaka-u.ac.jp

F. Arisaka

Life Science Center, College of Bioresource Science, Nihon University, 1866 Kameino, Fujisawa, Kanagawa 252-0880, Japan

1.2 Principle for Sedimentation and Diffusion

1.2.1 Sedimentation

Suppose we suspend some homogeneous fine grains of sand in water and stir and leave it still (Fig. 1.1). The boundary between the air and the solution is called “meniscus.” The sand will leave the meniscus and slowly sediment and the moving boundary will appear. Above the moving boundary, sand grains have sedimented down and are already gone. Below the boundary, the same concentration or the same number of grains per unit volume of sand is still there sedimenting with the same velocity. The speed of the moving boundary, v , is proportional to the acceleration of gravity, and the proportionality constant, s , will define the sedimentation coefficient of the sand particle.

$$v = sg \quad (1.1)$$

If all the sand particles have the same s -value, they sediment with the same velocity toward the bottom and the concentration at plateau region is kept constant. The particles that have reached at the bottom accumulate there.

Now, s is related to the mass, m , and specific volume, \bar{v} , of the particle and the density of water, ρ :

$$s = \frac{m(1 - \bar{v}\rho)}{f}, \quad (1.2)$$

where f is the frictional coefficient of the particle. The term $\bar{v}\rho$ is the excluded volume of the particle and $m\bar{v}\rho$ is the mass of the excluded water, leading to the

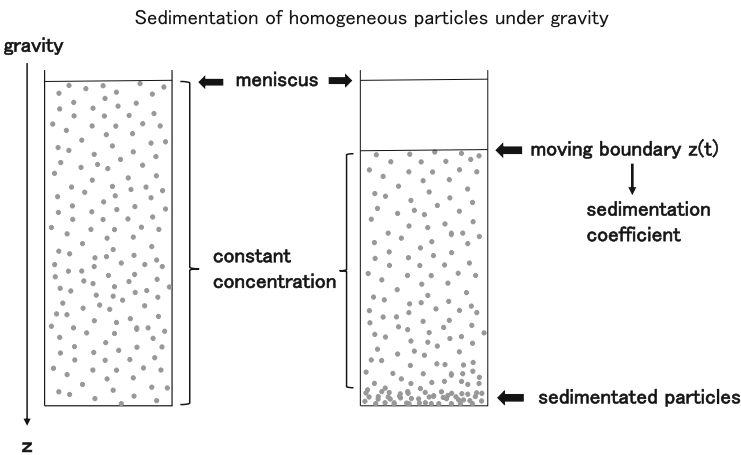


Fig. 1.1 Sedimentation of homogeneous grains in a cylinder under gravity

buoyancy. The term $m(1 - \bar{v}\rho)$ is called the buoyant mass. If the sand particles are not homogeneous, each size of the sand grain sediments with its own sedimentation coefficient, and we may observe the distribution of sedimentation coefficients.

Before invention of the analytical ultracentrifuge, Thé Svedberg measured the size distribution of colloidal gold which he was studying by the method as described above. In order to measure the position of the moving boundary precisely, he observed the boundary using a microscope. Eventually, Svedberg got interested in measuring the size of proteins which had been recognized to be very important in biological organisms. However, s -values of proteins are too small and do not sediment at all under the normal gravity due to the overwhelming diffusion. In order to let them sediment in spite of diffusion, the gravity has to be much increased, and he decided to utilize the centrifugal force of a centrifugation. Special devices, then, had to be developed in order to observe the moving boundary or the concentration gradient in the cell in a revolving rotor. Thus, Svedberg designed and constructed a prototype of analytical ultracentrifuge.

The velocity, v , of sedimentation of the moving boundary, r_b , is proportional to the centrifugal force, and the sedimentation coefficient is defined as the proportionality constant:

$$v = sr_b\omega^2, \quad (1.3)$$

where r_b is the position of the moving boundary from the center of revolution and ω is the angular velocity. It is noted that g in Eq. (1.1) is now replaced by $r\omega^2$, the acceleration of centrifugal force. The sedimentation coefficient is related to the mass of the particle, m , and the frictional coefficient, f :

$$s = \frac{m(1 - \bar{v}\rho)}{f} = \frac{M(1 - \bar{v}\rho)}{N_A f}, \quad (1.2a)$$

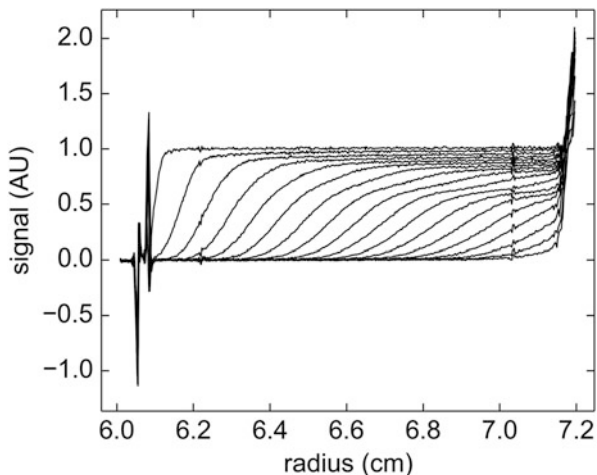
where N_A is the Avogadro's number, ρ is the density of the solvent, and M is the molar mass. s has the dimension of time and commonly used with the unit of S, where 1 S is 10^{-13} s. Simple classical mechanics treatment shows \bar{v} to be a specific volume, but more rigorous treatment of the transport process by nonequilibrium thermodynamics shows that it is a partial specific volume or

$$\bar{v} = \left(\frac{\partial V}{\partial m} \right)_{T,p}, \quad (1.4)$$

where \bar{v} is a volume increase of a solution of a large volume when 1 g of lyophilized protein or other solute molecules had been dissolved. If the concentration of the solute is low enough, it is close to the specific volume. From Eq. (1.3) or $(dr_b/dt) = sr_b\omega^2$,

$$\ln(r_b) = \ln(r_m) + s\omega^2 t \quad (1.5)$$

Fig. 1.2 Typical data of sedimenting boundary in sedimentation velocity experiment



so that

$$s = \ln(r_b/r_m) / (\omega^2 t),$$

where r_m denotes the position of the meniscus.

Svedberg noticed at the early stage of the development of his analytical ultracentrifuge (AUC) that the cell has to be sector shaped instead of rectangular, because the particle sediments in the direction of radius and if the cell is rectangular some particles will collide with the wall and the moving boundary will be distorted. The consequence of the sector-shaped cell is that the concentration of the solute at the plateau region, c_p , will gradually decrease due to the fact that the cross section of the flow of the solute will expand proportionally to the distance, r , from the center of revolution (Fig. 1.2):

$$C_p = C_0 e^{-2s\omega^2 t} \quad (1.6)$$

The analysis of moving boundary will be described more in detail when we introduce the Lamm equation which describes the time course of the concentration gradient in sedimentation velocity. r_b is then defined as the position of r , where the concentration is half that of the plateau region.

The value of sedimentation coefficient thus determined depends on the buffer conditions and temperature. The buffer condition changes the density and viscosity and the temperature mainly affecting the viscosity of water. In order to obtain the intrinsic physical parameter of the solute, the density and viscosity have to be corrected to reflect the experimental conditions.

It may be noted that in the above discussion, we are not looking at the behavior of each sedimenting molecule in solution but looking at the moving boundary or the concentration gradient at the boundary. All the information we extract concerning

the characteristics of the solute molecules are contained in the shape and its change during time course of the moving boundary. In fact, the moving boundary contains abundant information concerning homogeneity/heterogeneity, sedimentation coefficients and their distribution, diffusion coefficient and interactions between solute molecule, non-ideality, etc. Measurement of moving boundary is similar to the frontal analysis of the size exclusion chromatography.

1.2.2 Diffusion

Sedimentation coefficient and frictional coefficient are related through Eq. (1.2a). Now, there is a simple relation between diffusion coefficient and frictional coefficient for ideal solution which is called the Einstein-Sutherland equation:

$$D = \frac{RT}{N_A f} \quad (1.7)$$

Replacing f in Eq. (1.2a) with f in Eq. (1.7) will give the Svedberg equation:

$$\frac{s}{D} = \frac{M(1 - \bar{v}\rho)}{RT} \quad (1.8)$$

This equation indicates that if we have the values for s and D , we can determine the molar mass, M , with the advance knowledge of \bar{v} and ρ . The molar mass thus determined does not depend on the shape of the molecule as the equation implies.

In the case of non-ideality, D can be expressed as

$$D = \frac{RT}{N_A f} \left\{ 1 + C \frac{\partial \ln \gamma}{\partial C} \right\} \quad (1.9)$$

and the corresponding Svedberg equation is

$$\frac{s}{D} = \frac{M(1 - \bar{v}\rho)}{RT \left\{ 1 + C \frac{\partial \ln \gamma}{\partial C} \right\}}, \quad (1.10)$$

where γ is the activity coefficient of the solute.

Now, assume a cell of uniform cross section with infinite length and that a sharp concentration gradient or boundary is present at $x = 0$ at time $t = 0$ (Fig. 1.3). The time course of the change of concentration gradient can be predicted by the Fick's second law (diffusion equation):

$$\left(\frac{\partial C(x, t)}{\partial t} \right)_x = D \left(\frac{\partial^2 C(x, t)}{\partial x^2} \right)_t, \quad (1.11)$$

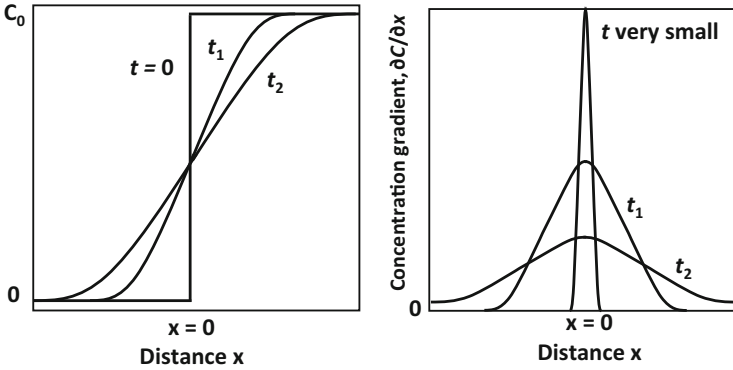


Fig. 1.3 Change of concentration gradient of solute due to diffusion

where D is the translational diffusion coefficient. Equation (1.6) can be solved with the initial condition and boundary condition. Under these conditions of free diffusion, the solution of Eq. (1.6) is

$$C(x, t) = \frac{C_0}{2} \left\{ 1 - \frac{2}{\sqrt{\pi}} \int_0^{x/2\sqrt{Dt}} e^{-y^2} dy \right\} \quad (1.12)$$

and the derivative of $C(x, t)$ with respect to x is simply a Gaussian “error” curve:

$$\left(\frac{\partial C(x, t)}{\partial x} \right)_x = \frac{C_0}{2\sqrt{\pi Dt}} e^{-x^2/4Dt}, \quad (1.13)$$

where c_0 is the concentration of the solute at $t = 0$. We can get the gradient either by calculating from the experimental concentration gradient data or measure the gradient by traditional so-called schlieren optical system. The height of the bell-shaped curve, H , is given by

$$\left(\frac{\partial C(x, t)}{\partial x} \right)_{x=0} = \frac{C_0}{2\sqrt{\pi Dt}} = H \quad (1.14)$$

and

$$\left(\frac{C_0}{H} \right)^2 = 4\pi Dt \quad (1.15)$$

We can thus determine D by plotting $(C_0/H)^2$ with respect to t . There is a special cell, synthetic boundary cell, which can be used to form a sharp boundary to determine the diffusion coefficient by the method as described above. In current practice, both

sedimentation coefficient and diffusion coefficient are determined by direct curve fitting to the Lamm equation solution to the raw data of sedimentation velocity.

1.3 Sedimentation Velocity

1.3.1 Lamm Equation

As soon as the solute molecules leave the meniscus and start to sediment, a concentration gradient will appear. In the concentration gradient (moving boundary), sedimentation and diffusion take place simultaneously. It was Ole Lamm, a Ph.D. student of Thé Svedberg, who reported a partial differential equation which describes the time course of the concentration gradient of the solute in sedimentation velocity (Lamm 1929):

$$\left(\frac{\partial C}{\partial t}\right)_r = -\frac{1}{r} \left\{ \frac{\partial}{\partial r} \left[s\omega^2 r^2 C - D r \left(\frac{\partial C}{\partial r} \right)_t \right] \right\} \quad (1.16)$$

This equation, called the Lamm equation after Ole Lamm, precisely describes the time course of the sedimentation together with diffusion. Detailed derivation of the Lamm equation is described elsewhere. Due to the consideration of the sector-shaped cell, the right-hand side of the equation is somewhat complicated, but, basically, it consists of two terms in the brackets []. The first term has the coefficient s , and the second term contains D . The former describes sedimentation and the latter diffusion. In current methods of SV analysis, s and D are determined by nonlinear least squares curve fitting to the raw data.

Equation (1.16) assumes that s and D are constants (i.e., there is no hydrodynamic non-ideality) under the same conditions. The measured s - and D -value are usually corrected to a standard condition which is traditionally in water at 20 °C, $s_{20,w}$, $D_{20,w}$. If the actual measurements were made in a buffer solution at temperature T , $s_{T,b}$, (1.2a) and (1.7) contain the frictional coefficient, which is related to the viscosity of the solvent by the Stokes law:

$$f = 6\pi\eta R_s, \quad (1.17)$$

where R_s is the Stokes radius and has been worked out for particles of various shapes. In any event, it is directly proportional to the viscosity of the solvent. The measured $s_{T,b}$ and $D_{T,b}$ are, therefore, corrected for viscosity and the density of the solvent:

$$s_{20,w} = \frac{(1 - \bar{v}\rho)_{20,w}}{(1 - \bar{v}\rho)_{T,b}} \frac{\eta_{T,b}}{\eta_{20,w}} s_{T,b} \quad (1.18)$$

$$D_{20,w} = \frac{293.1}{T} \frac{\eta_{T,b}}{\eta_{20,w}} D_{T,b} \quad (1.19)$$

Correction for viscosity is mainly due to the temperature dependence of that of water. For example, the viscosity of water at 4°C is about 1.3 times larger than that of water at 20°C. The s - and D -values thus corrected are known to depend on the concentration of the solute and need to be extrapolated to zero concentration in order to obtain the real intrinsic physical parameter of the solute $s_{20,w}^0$. For common spherical soluble proteins, extrapolation to zero concentration may not be necessary if the concentration is below 1 mg/mL or so. However, care has to be taken for extremely elongated proteins such as triple-helical collagen or highly negatively or positively charged molecules such as nucleic acids. In fact, the s -value of nucleic acids has a much higher concentration dependence than proteins and has to be measured at very low concentration. Fortunately, nucleic acids, DNA and RNA, have much higher extinction coefficients than proteins, and, as a result, they can be measured at much lower concentration. Extinction coefficient of nucleic acids is about 20 times larger than those of proteins. Much less frequently, sedimentation coefficients may decrease as the concentration decreases. In such a case, subunit dissociation may be anticipated.

1.3.2 Relationship Between s and M

The molar mass, M , of the sedimenting particle can be estimated by Svedberg Eq. (1.18), which requires the s - and D -values. The s -value can be determined rather accurately with the error of one or two percent. On the contrary, D -values are more difficult to evaluate precisely, and they have been frequently obtained from DLS measurement and combined with the s -value from SV experiments. However, recent software, such as $c(s)$ analysis in SEDANAL, SEDFIT, or ULTRASCAN, utilizes the relationship of D and f/f_0 , called the scaling law:

$$D(s) = \frac{\sqrt{2}}{18\pi} kTs^{-1/2} (\eta(f/f_0)_w)^{-3/2} ((1 - \bar{v}\rho) / \bar{v})^{1/2} \quad (1.20)$$

The rationale of using this equation for analysis is discussed by Peter Schuck. In $c(s)$ analysis, a common value for f/f_0 value is assumed, but there is another mode of analysis $c(s, f/f_0)$ in SEDFIT or 2DSA in ULTRASCAN, where s and f/f_0 are independently fitted for each molecular species. SEDANAL fits directly for s and D for each species with or without constraints relating the frictional coefficients of each component.

1.3.3 Molecular Shape and f/f_0

Molecular shape may be discussed based on the frictional ratio, f/f_0 . The frictional ratio, obtained from the SV analysis, may be related to the molecular shape of the

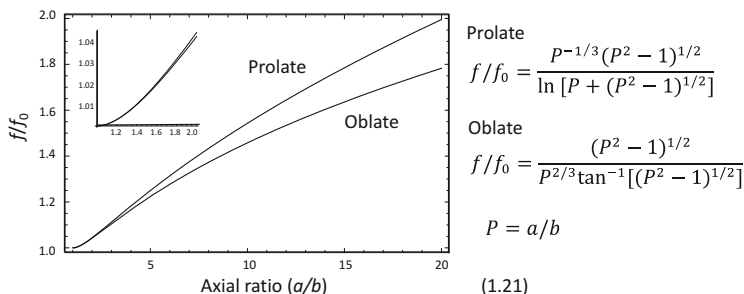


Fig. 1.4 Relationship between axial ratio and frictional ratio

assumed prolate, oblate, or rod, through Perrin's equations (Fig. 1.4). As shown in Fig. 1.4, a small increase of f/f_0 increases the axial ratio quite a bit, but a large change in the axial ratio does not affect the f/f_0 very much, which is the rationale of using Eq.(1.21) independent of the molecular species. Note that spherical protein will give the f/f_0 of about 1.2 instead of 1.0, which is because f_0 is estimated for a protein without solvation, whereas the experimentally determined f includes solvation. We cannot discuss the molecular shape in detail but can decide if the molecule is close to sphere or elongated (or flattened). For example, native triple-helical collagen has a large f/f_0 value, larger than 2.

1.3.4 Sedimentation Coefficients Estimated from the X-ray Structure of the Proteins

If the atomic structure of a protein is known, one can estimate the hydrodynamic values including the sedimentation coefficient and diffusion constant. Although it is not so simple to predict the structure from the sedimentation coefficient, if a number of possible model structures are available, one could assess each structure by estimating each s -value and judge which model would fit the measured s -value (Rocco and Byron 2015).

1.4 Sedimentation Equilibrium

When solution is centrifuged at a relatively low speed as compared with that of the SV experiments, both sedimentation and diffusion contribute significantly to the concentration distribution. As a result, the moving boundary which we see in SV experiments will not be seen. Instead the concentration of the solute at the meniscus will decrease and that at the bottom will increase and eventually reach the equilibrium, when sedimentation and diffusion are balanced. The resultant